Springer

KSME

Journal of Mechanical Science and Technology 31 (2) (2017) 937~948
www.springerlink.com/content/1738-494x(Print)/1976-3824(Online)
DOI 10.1007/s12206-017-0146-9

Performance evaluation of a twin-shaft gas turbine engine in mechanical drive service †

Mohammadreza Tahan, Masdi Muhammad* and Z. A. Abdul Karim

Department of Mechanical Engineering, Universiti Teknologi PETRONAS, 32610 Bandar Seri Iskandar, Malaysia

(Manuscript Received February 21, 2016; Revised August 11, 2016; Accepted September 5, 2016)

Abstract

This study aimed at quantifying the effect of mechanical load on the performance of an 18.7 MW offshore gas turbine engine. The targeted engine is of two-shaft free power turbine configuration that operates as a mechanical driver for a process compressor in the gas compression service. The study is a part of a comprehensive performance health monitoring program to address the diagnostic and prognostic requirements in oil and gas offshore platforms and is motivated by the need to provide in-depth knowledge of the gas turbine engine performance. In this work, only the context of some design point key performance parameters and a limited set of collected operational data from the gas turbine in the real plant are available. Therefore, three major tasks, namely design point calculation, characteristic map tuning and off-design performance adaption, were needed to be performed. In order to check the validity of the proposed model, the obtained simulation results were compared with the operational data. The results indicate the maximum inaccuracy of the proposed model is 3.04 %. Finally, by employing the developed model, the engine capability for power generation when exposed to various load speeds is investigated. The obtained result demonstrates at the maximum gas generator speed, every 3 % decrease in mechanical speed leads to 1 % decline in the gas turbine power output. Moreover, when the gas turbine operates under design power load and mechanical speed is lower than 80 % of design speed, every 1 % decrease in load speed results in 0.2 % loss in thermal efficiency. The established relationship will assist proper assessment of mechanical drive gas turbines for performance health monitoring.

Keywords: Part-load; Performance analysis; Analytical simulation; Component map; Gas turbine; Process compressor

1. Introduction

The recent increase of using high-horsepower industrial machinery in locations where steam turbine drivers are not practical resulted in a renewed interest in heavy-duty gas turbine engines. The current applications of this versatile item of turbomachinery mainly include driving electric generators for power generation, multi-stage compressors for oil field gas reinjection service, transport compressors in gas treatment and distribution plants, and refrigeration compressors for LNG liquefaction service. Due to continuous variation in the power and speed demands, off-design performance simulation of gas turbine engines plays an important role in equipment healthy operation and maintenance optimization, particularly in mechanical drive applications.

The last 20 years have seen a large development of gas turbine technology. However, with privatization and intense competition in the industry, there is a strong incentive for gas turbine operators to increase the machine efficiency and minimize performance deterioration, as this directly affect profitability. Toward this goal, various analytical and experimental approaches were employed to simulate the operation of a gas turbine.

Since one of the major problems in this area is the lack of available component data, many studies have focused on the component map generation. Conventional stage stacking approach [1], scaling technique [2], and regression adaption [3] are the most commonly introduced family of methods to address this problem.

The approaches adopted in the majority of gas turbines to achieve the targeted load usually relies on controlling fuel flow and adjusting compressor Variable guide vanes (VGVs). Additionally, variable geometry compressors enable engine exhaust temperature to be controlled, and hence, improves the cycle efficiency in off-design operation. However, it should be noted that the shape of component characteristic curves varies for every degree of VGV closure, which is a challenge in part load simulation. Special efforts are made to update the gas turbine component that employs VGVs. Muir et al. [4] and Kim et al. [5] developed a compressor model based on a modified stage stacking method, which includes modulating the VGVs. Haglind [6] studied the effects of VGVs on engine performance in an approximate way using the technique pro-

*Corresponding author. Tel.: +605 3687058, Fax.: +605 3687058
E-mail address: masdimuhammad@petronas.com.my
† Recommended by Associate Editor Tong Seop Kim

posed by the gas turbine performance simulation software GASTURB 11 [7].

To conduct gas turbine performance analysis, the programs to calculate thermodynamic cycle or component matching analysis are widely investigated by many researchers. Saravanamuttoo and MacIsaac [8] employed cycle programming to the model pipeline gas turbine to predict engine performance and calculate principle thermodynamic parameters for diagnostics. Razak [9] extensively investigated the process of component matching to simulate the off-design performance of various types of gas turbine engines.

Another category of research efforts was carried out to study the component map generation and part load performance prediction simultaneously. Gobran [10] developed the off-design performance of Solar Centaur-40 engine by introducing various approaches to calculating design point, scale characteristic maps, and simulate part load. Spina [1] modeled the performance of a gas turbine using generalized stage performance curves through stage stacking, where the value of unknown parameters reproducing the overall thermodynamic and performance data are calculated through a reiterative process of cycle programming. Visser and Broomhead [11] developed a gas turbine simulation program, which is an off-design model to simulate gas turbine engines. Recently, Rashidzadeh et al. [12] developed a design and off-design model for SGT-600 twin-shaft gas turbine for mechanical drive applications, where the characteristic curves of components are derived using numerical simulations and are validated with experimental data. Bahrami et al. [13] also developed a dynamic model for long-term simulation of a heavy duty gas turbines. The model includes the essential control algorithm and presents the most common outputs and important intermediate variables of the gas turbine.

This paper is aimed at performance analysis of two-shaft gas turbine in mechanical applications. In this engine configuration, the rotational speed of power turbine, known as mechanical speed, is affected by driven load. Unlike the electrical generator application that needs constant power turbine speed, in mechanical drive cases, the driven equipment speed may vary by load. For example, during dense phase operation of process compressors because of high suction pressures, the driven compressor speed may drop. Therefore, it is worthwhile to investigate the trend of power in various power turbine speeds. To achieve this goal, an off-design performance analysis approach of gas turbine engine considering its configuration and load condition is proposed. The model was constructed using scaling technique to estimate the performance maps of the machine components. Thermodynamic cycle programming was employed to calculate the key thermodynamic parameters at the design point. A component-matching process was adopted to calculate the part load condition of the gas turbine. Then, this model was verified using the obtained experimental data. And finally, the variation of gas turbine power output with power turbine speed was investigated.

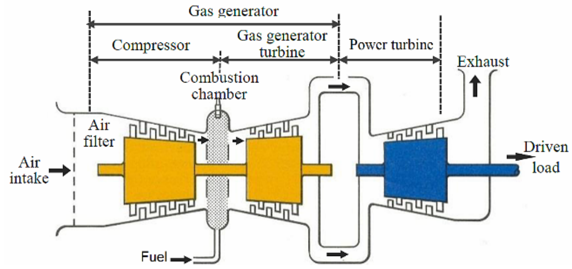

Fig. 1. Sketch of the studied gas turbine engine.

2. Case study

The case study involves a two-shaft gas turbine operating as a mechanical drive in an offshore oil and gas plant in the east of Peninsular Malaysia. The engine corresponds to an industrial gas turbine of about 18.8MW ISO power rating. This machine is utilized to drive compressors with a significant variation in the speed with the power demand. In such applications, the power turbine can run at the speed of the load and the gas generator can operate at its maximum speed.

2.1 Engine configuration

In this two-shaft machine, the expanding part is split into two separate turbines. The first turbine, named gas generator turbine, drives the compressor, and the second one, called the power turbine, drives the load. The gas generator functions to produce high-pressure and high-temperature gas for the power turbine. There is no mechanical coupling between these two components, however, strong fluid or aerodynamic coupling exists between them. A schematic diagram of the studied engine is given in Fig. 1.

2.2 Operating strategy

The control strategy of the studied gas turbine involves a set point of driven compressor. The control system moves the engine towards this set point, which can assume to be power, mass flow rate, discharge pressure, or rotational speed of the driven compressor. In addition, this engine is controlled by limiting the following conditions, which are considered to mitigate probable operating risks: 1) The gas generator temperature is limited, to prevent the engine from overheating, 2) the gas generator and power turbine speed are controlled to prevent the rotating parts from being over-stressed, and finally 3) the upper limit on aerodynamic or non-dimensional speed prevents the stalling and surging of the compressor at high speeds. Typically, the two main tools are used to achieve the required set point, namely, 1) fuel flow control, and 2) Variable guide vanes (VGVs) setting. Although turbine power can be constantly adjusted by continuous controlling of the fuel flow, setting this parameter alone may cause many problems in the engine, including over-speeding and overheating. Therefore, using VGVs at the inlet and early stages of the compressor is an alternative method to improve the off-design

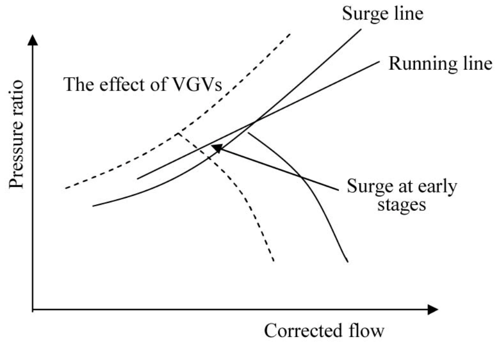

Fig. 2. Effect of variable guide vanes closure on a compressor characteristic curve.

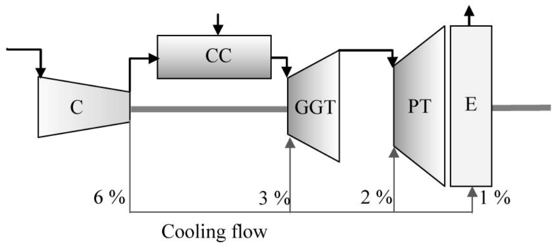

Fig. 3. Sketch of gas turbine bleeding for cooling purposes.

performance of the gas turbine. Here, in targeted engine, the variable guide vanes of the inlet and first six stages of the compressor are employed to accomplish this duty. The variation of engine performance due to VGVs adjustment can be traced to the change in compressor characteristic curve. The dotted line in Fig. 2 illustrates the effect of VGVs closure on the compressor map.

Closing the VGVs prevents the running line and surge line to intersect at low compressor speeds, and consequently, the engine can be started, as observed in Fig. 2. Furthermore, at high compressor speeds, the front stages start to choke, forcing the back stages to stall. Opening the stators of the front stages allows more inward flow and prevents stalling at back stages.

In the case study gas turbine, the air bleeding is also predicted to supply coolant and protect the machine against surges in very low speeds. Blow-off reduces the flow to the back stages of compressor that leads to air velocity reduction in these stages and prevents choking. However, blow-off yields waste of energy and this process is thus only employed during start-up and shutdown. Since the goal of this research is to analyze the engine operation during loading, not starting, we assumed that bleeding is not used as engine control method and the blow-off valves are considered for cooling purposes only. Accordingly, in order to simulate the effect of air bleeding, 6 % of the air is extracted from the compressor. Fig. 3 indicates that 3 % of this bleed air is injected into the gas generator turbine and 2 % is injected into the power turbine for similar usage in this component for mid frame cooling, trust balance, and engine sump seals and 1 % is used for high-speed coupling cooling.

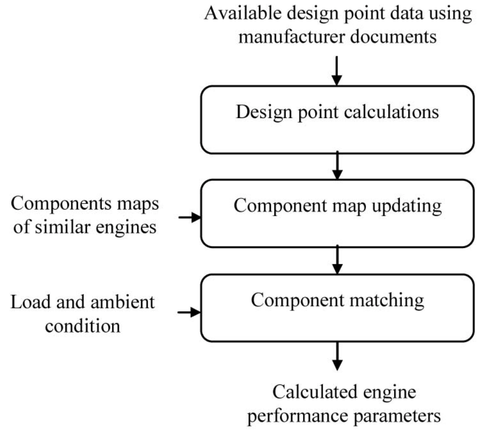

Fig. 4. Procedure for part-load performance evaluation.

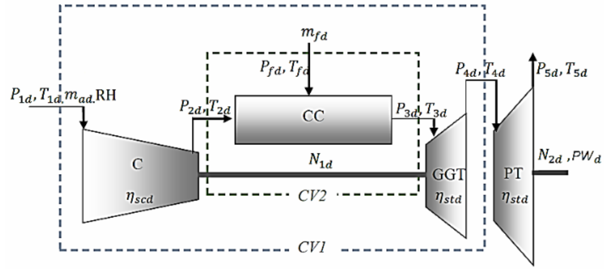

Fig. 5. Sketch of considered control volumes.

3. Engine performance modeling

In mechanical drive applications, the satisfactory operation of the gas turbine engine at part-load conditions is of paramount significance since these conditions are commonplace during load changes. The part load performance of the gas turbine engine is governed by the performance characteristics of its consistent components, namely compressor, combustor, and turbines, and by the laws of compatibility of pressure ratio, rotational speed and mass flow rate, which determine the interaction or matching between them. In this investigation, the only available information includes some design point's key performance parameters and a limited set of experiment collected data, therefore, the procedure illustrated in Fig. 4 is proposed to perform a part load performance evaluation.

3.1 Design point calculations

The main objective of the design point calculation is to obtain required data for components map scaling. The data, indicated in Fig. 5, include thermodynamic properties such as P and T at different gas path points, compressor inlet airflow rate, fuel flow rate, component isentropic efficiencies, gas generator speed, power turbine speed, and the net power output. The unavailable parameters that need to be calculated includes T_{2d} , P_{3d} , T_{3d} , P_{4d} , P_{5d} , m_f . In order to calculate these parameters, the thermodynamic energy analysis has been employed. All the design properties are calculated through the thermodynamic calculations presented in Appendix A.2.

3.2 Component map tuning

Component maps exhibit the relationship between corrected rotational speed, Eq. (1), corrected mass flow rate, Eq. (2), pressure ratio, Eq. (3), and isentropic efficiency Eq. (4).

$$N_{cor} = \left(N / \sqrt{T_i} \right) \tag{1}$$

$$w_{cor} = \left(w\sqrt{T_i} / P_i \right) \tag{2}$$

$$PR = \left(P_{out} / P_{in} \right) \quad \text{(for compressor) or}$$

$$PR = \left(P_{in} / P_{out} \right) \quad \text{(for turbine)} \tag{3}$$

$$\eta = \left(\Delta h_{is} / \Delta h_{real} \right) \quad \text{(for compressor) or}$$

$$\eta = \left(\Delta h_{real} / \Delta h_{is} \right) \quad \text{(for turbine)} \tag{4}$$

where N, w, T_i and P_i are the rotational speed (rpm), inlet mass flow rate (kg/s), inlet temperature (K), and inlet pressure to the compressor or turbine (kPa), respectively. In order to simplify using performance maps, it is common to normalize corrected speed, corrected mass flow, pressure ratio and isotropic efficiencies using design point values.

As discussed earlier, the compressor and turbine performance curves are proprietary of gas turbine manufacturers and are usually not available to end-users. To address this problem in the present research, characteristic maps of similar compressors and turbines presented by Lazzaretto and Toffolo [14] are firstly selected. The scaling method, which is a simple yet effective technique, is employed to match these maps for the targeted engine. Scaling is the process of multiplying all the values of an original curve by a specific factor to obtain the component characteristics of a similar engine. This factor should be chosen so that the design point of the reference engine becomes similar to the design point of the targeted engine. According to what has been proposed by Sellers and Daniele [15] and Kong et al. [16], each parameter could be scaled using Eqs. (3)-(7).

$$PR_{pm-t} = \frac{PR_{d-t} - 1}{PR_{d-r} - 1} * \left(PR_{pm-r} - 1 \right) + 1 \tag{5}$$

$$\left(w_{cor} \right)_{pm-t} = \frac{\left(W_{cor} \right)_{d-t}}{\left(W_{cor} \right)_{d-r}} * \left(w_{cor} \right)_{pm-r} \tag{6}$$

$$\eta_{pm-t} = \frac{\eta_{d-t}}{\eta_{d-r}} * \eta_{pm-r} \ . \tag{7}$$

Additionally, the effects of VGVs on compressor characteristic curves are estimated using the methodology introduced by Haglind [6]. In the current research, it is assumed at the design point where the actuator is fully open, guide vane angle $\Delta\alpha$ is zero, and for any other given angle, the characteristic parameters can be achieved using Eqs. (8)-(10):

$$PR_{VGV} = (PR_{pm-t} - 1)\left(1 + \frac{c_2 \Delta\alpha}{100} \right) + 1 \tag{8}$$

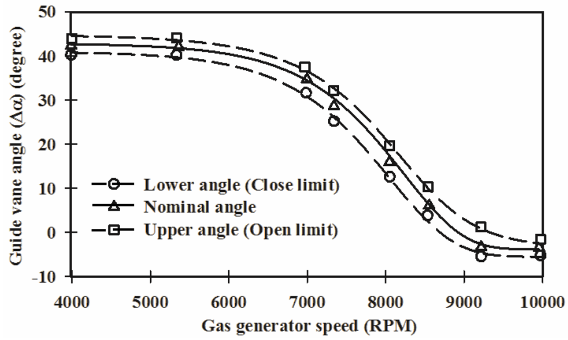

Fig. 6. Compressor variable guide vanes schedule.

$$\left(W_{cor} \right) = (W_{cor})_{pm-t} \left(1 + \frac{c_1 \Delta\alpha}{100} \right) \tag{9}$$

$$\eta_{VGV} = \eta_{pm-t} \left(1 - \frac{c_3 \Delta\alpha^2}{100} \right) \tag{10}$$

where c_1, c_2, c_3 are the constant coefficients and the verified values are 1, 1 and 0.01, respectively, as per GASTURB 11 [7]. All VGVs are mechanically ganged together, and their angular pitches are adjusted in response to the change in the temperature of compressor inlet or speed of the gas generator. Because of inaccessibility to manufacturer design data corresponding to the variable geometry compressor operation, the approximate VGVs schedule for the targeted gas turbine is achieved using experimental data. Since the gas turbine is installed in a tropical area where the ambient temperature does not vary substantially, the angular position of the VGVs is scheduled using the gas generator corrected speed. However, the slight variation in inlet air temperature causes a bound guide vane angle at every gas generator speed, as shown in Fig. 6. In this study, the nominal angle that corresponds to normal ambient temperature of 301.95 °K is applied.

3.3 Off-design modeling using matching process

A methodology for part-load performance analysis of a two-shaft gas turbine engine using the matching process is introduced in this section. During the steady-state operation of the engine without loading or under loading, certain matching constraints must be satisfied. Since this research intends to evaluate the influence of required power and mechanical speed on gas turbine performance, the power output, compressor inlet temperature, compressor inlet pressure, ambient humidity, and power turbine speed (mechanical speed) are assumed to be the input variables. Appendix A.3 presents the proposed matching procedure for the case study gas turbine in order to develop an off-design model.

4. Results and discussion

To investigate the potential of the proposed performance evaluation model, a comparison between simulation results

Table 1. Complete set of design point performance parameters of case studies gas turbine.

Parameter	Description	Value	Unit
Available data			
T_{1d}	Gas generator inlet temperature	301.95	K
P_{1d}	Gas generator inlet pressure	1.013	bar(a)
RH	Relative humidity	90	%
P_{2d}	Compressor output pressure	17.27	bar(a)
N_{1d}	Gas generator speed	9160	rpm
N_{2d}	Output shaft speed	3523	rpm
m_{ad}	Air flow	60.51	kg/s
T_{4d}	Gas generator exhaust temperature	807.78	K
T_{5d}	Power turbine exhaust temperature	541.67	K
η_{scd}	Compressor isentropic efficiency	0.81	-
η_{std}	GGT and PT isentropic efficiencies	0.85	-
PW_{outd}	Output power	18669	kW
Derived data			
T_{2d}	Air temperature at compressor outlet	470.82	K
P_{3d}	Combustor outlet pressure	16.74	bar(a)
T_{3d}	Combustor outlet temperature	1175.6	K
P_{4d}	Gas generator outlet pressure	4.15	bar(a)
P_{5d}	Exhaust pressure	1.0426	bar(a)
λ_d	Fuel-air mass ratio	0.0189	-
m_{fd}	Fuel flow rate	1.145	kg/s

obtained using this model and the experiment data collected from an actual engine during the off-design operation is presented here. The independent variables are assumed ambient temperature and pressure, power output, and power turbine rotational speed. To conduct the analysis, the following nominal assumptions of the decision variables are considered. The value of ΔP_1, ΔP_{CC} and ΔP_{ED} are assumed 1 %, 2 % and 2.5 %, respectively. The heat loss of the combustion chamber ΔQ_{CC} is considered 2 %. At standard atmospheric condition, the result of the air molar analysis (%) is $73.77N_2, 19.6O_2$, $0.0285CO_2, 6.6H_2O$. The gas turbine operates in an offshore plant at a tropical region, thus, the average inlet air humidity at the period of data collection is considered 90 % and the inlet air composition is updated. Using gas turbine mechanical datasheet, fuel temperature (T_f), lower heating value $(\overline{LHV_f})$, and average fuel molecular weight (mw_f) are considered 305.15 °K, 37.38 MJ/kg, and 22.46, respectively. The fuel molar analysis (%) at the design condition is also considered $0.31N_2$, $11.90CO_2$, $0.01H_2O$, $76.92CH_4$, $6.91C_2H_6$, $3.8C_3H_8$ and $0.25C_4H_{810}$.

Table 2. The maximum percentage error in the compared variables.

Variable	Description	Maximum error %
PR_C	Compressor pressure ratio	2.52
T_4	GGT outlet temperature	3.04
P_4	GGT outlet pressure	2.26
N_1	GGT rotational speed	1.81
m_f	Fuel mass flows rate	2.19

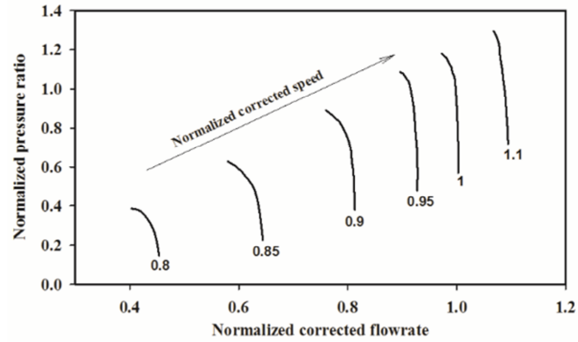

Fig. 7. Compressor characteristic map, normalized pressure ratio vs normalized corrected flowrate.

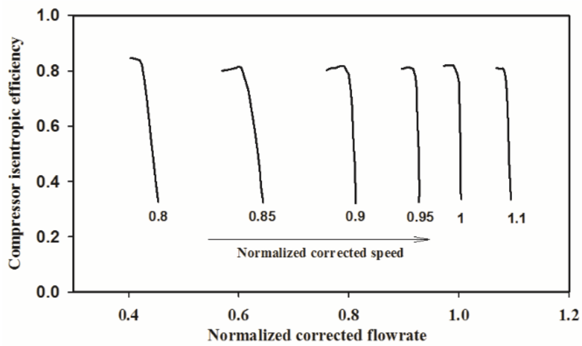

Fig. 8. Compressor characteristic map, efficiency vs normalized corrected flowrate.

Table 1 shows all available and derived necessary design parameters achieved using the proposed approach presented in Sec. 3.1.

The characteristic curves of GE LM 2500+ engine, which is presented by Lazzaretto and Toffolo [14], are chosen as the similar turbine curves. In order to read the compressor performance curves, the β lines approach, is employed. Appendix A.1 gives more additional information about the procedure of using this method. Scaling technique is employed to tune the characteristic maps using design point values based on the methodology presented in Sec. 3.2. The effect of VGVs that incorporates variable geometry angle is also considered in the modeling. Figs. 7-10 show the obtained compressor and power turbine characteristic maps.

Then, by using the component matching process introduced

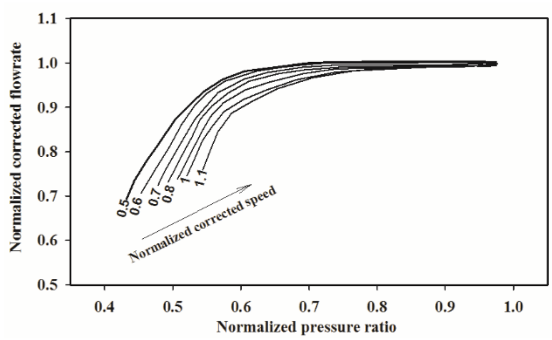

Fig. 9. Power turbine characteristic map, normalized corrected flowrate vs normalized pressure ratio.

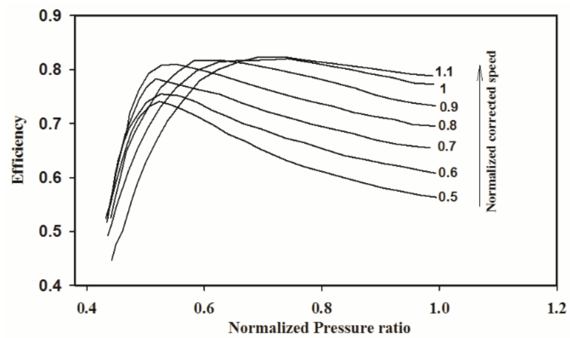

Fig. 10. Power turbine characteristic map, efficiency vs normalized pressure ratio.

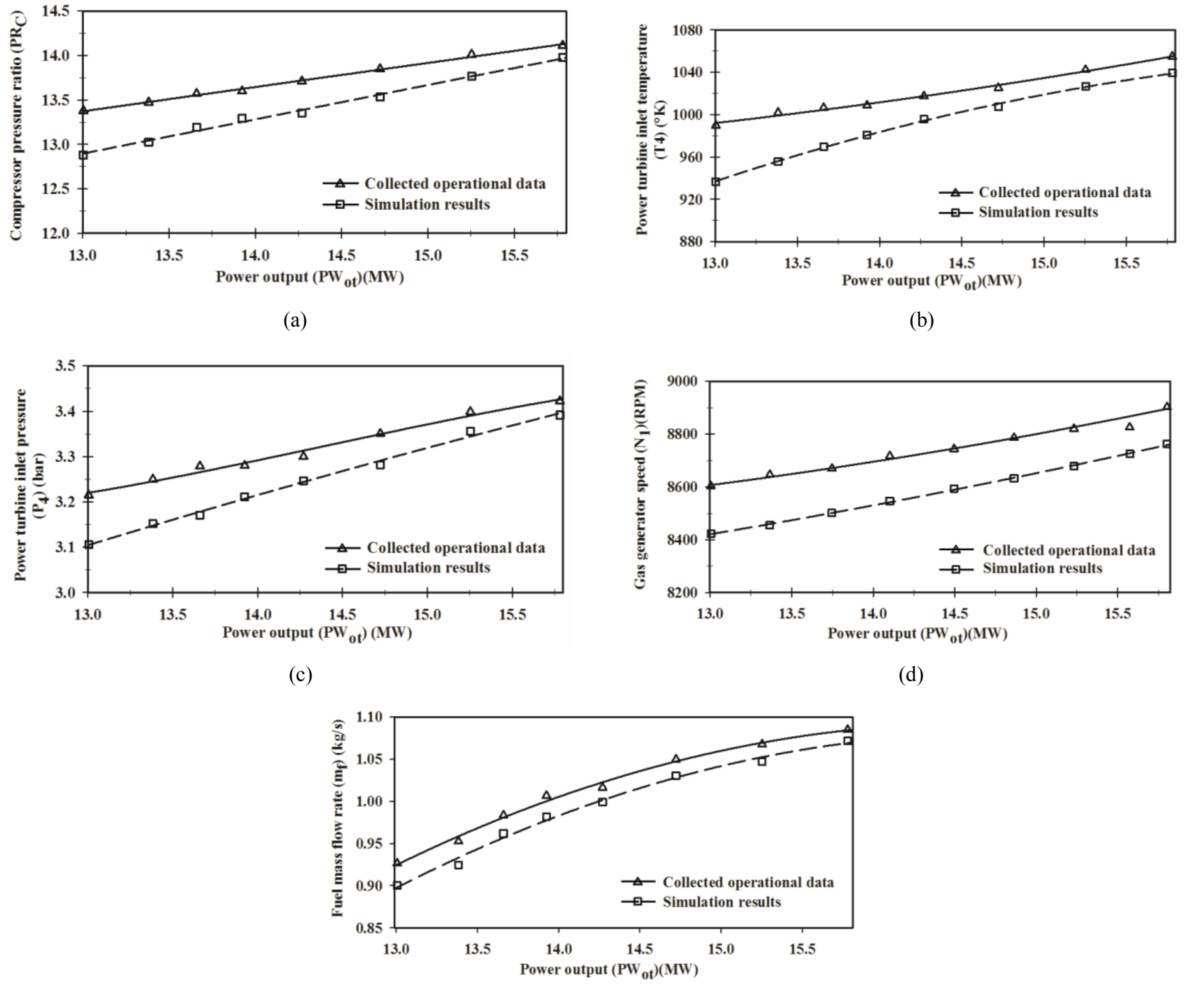

Fig. 11. A comparison between collected operational data and simulation result: (a) Compressor pressure ratio versus power output; (b) GGT outlet temperature versus power output; (c) GGT outlet pressure versus power output; (d) GG rotational speed versus power output; (e) fuel mass flow rate versus power output.

earlier, off-design simulation is carried out. Table 2 indicates the maximum percentage errors in the compared variables. A comparison between the results of simulation and operationally collected data in partial load analysis is also presented in Fig. 11. In all these computations, the ambient temperature and pressure are considered constant and equal to average daily plant ambient temperature and pressure, i.e. 301.95 °K and 1.013 bar(a), respectively. The satisfactory accuracy threshold is assumed 3 % for all required checks in the off-design simulation.

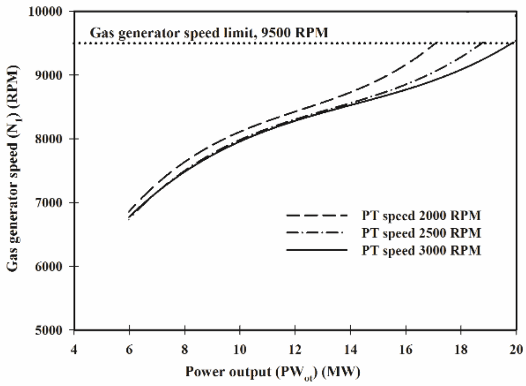

Fig. 12. Required speed of the gas generator versus required power at different rotational speeds.

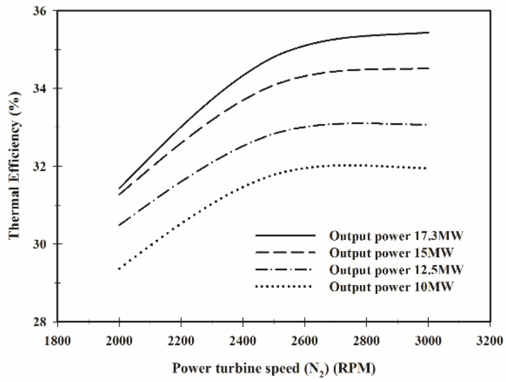

Fig. 13. Gas turbine thermal efficiency versus mechanical speed at various power outputs.

As illustrated, the results of the simulation are acceptable. The maximum percentage error is 3.04 %, which corresponds to the gas product temperature at the combustion chamber outlet. This phenomenon is mainly attributed to the approximation considered using combustion charts. Additionally, the accuracy of the model is significantly dependent on the gas turbine operating points. At the region far from a design point, the model accuracy decreases significantly. This is mainly because scaling technique is based on design points matching, and for other points gives a rough estimate of components characteristic.

In mechanical drive applications such as process compressors, speed and required power of the driven equipment have a substantial effect on the performance of gas turbine engine. Therefore, in next step, it is worth to investigate the influence of load variation on the gas turbine operation.

In Fig. 12, the required speed of the gas generator is drawn as a function of required power output for three different rotational speeds of driven equipment. In this figure, the corresponding curve of maximum power turbine speed, i.e. 3000 RPM, is of particular interest since this condition typically corresponds to the maximum load on the engine. As is observable in Fig. 12, there is an increase in gas turbine output power at higher gas generator speeds. This is mainly due to increase in air flowrate and fuel flowrate that consequently leads to an increase in the combustion airflow. In addition, it has been observed that the rate of increase in fuel flow is greater than increase in airflow. Therefore, the air-fuel ratio decreases and consequently the combustion temperature rises. Moreover, the compressor pressure ratio has increased that generally improves the gas power.

Another issue that can be seen in Fig. 12 is that at a specific gas generator speed, say 9000 RPM, the gas turbine output power is dependent on power turbine rotational speed, where the increase in power turbine speed improves the gas turbine power output. Fig. 12 shows, a decrease of gas turbine speed from 3000 RPM to 2100 RPM, i.e. 30 %, yields to approximately 10 % decline in gas turbine output power. This is mainly owing to the change in power turbine efficiency, where according to gas turbine non-dimensional characteristic curves, this value increases at higher rotational speeds.

Moreover, at higher gas generator speeds, the difference between powers produced at different power turbine speeds increases. The reason for this fact is that at higher compressor pressure ratio, the difference between the power turbine isentropic efficiencies increases more intensively, as is observable in Fig. 10. Moreover, the maximum achievable power declines when the rotational speed decreases because the gas generator speed reaches its maximum limit, i.e. 9500 RPM, sooner. It is, therefore, necessary that the driven load operates at relative speeds close to design speed.

Fig. 13 illustrates the variation of gas turbine thermal efficiency with the mechanical rotational speed at four power loads. As can be seen, for a given power output, increase in mechanical speed leads to higher thermal efficiency. This is mainly because of the improvement in power turbine efficiency at higher non-dimensional speeds, as can be seen in Fig 10. However, since the power turbine isentropic efficiency does not change noticeably with the variation of power turbine non-dimensional speed, at higher power turbine rotational speed the efficiency curve is relatively flat.

Another issue that can be seen in Fig. 13 is that at a particular power turbine rotational speed, the efficiency improves with the increase of useful power output. For example, at the mechanical speed of 3000 RPM, the overall thermal efficiency decreases by 10.9 % when the load power decreases to 10 MW from 17.3 MW. This is because gas generator speed and subsequently the compression ratio of the compressor and the temperature at turbine entrance increase when required power increases. This fact demonstrates that gas turbine engines are most efficient for high load conditions. To improve the thermal efficiency at low power outputs, one possible option is employing VGVs. In single-shaft gas turbines, the compressor's VGVs can be employed to control the airflow and maintain turbine exit temperature at its design value. However, in a two-shaft engine with a free power turbine, as our case study here, the exhaust gas temperature at off-design conditions can be maintained by using a variable geometry power turbine. Since the case study engine is a fixed geometry power turbine, in conditions that significant power decrease is desired, it can

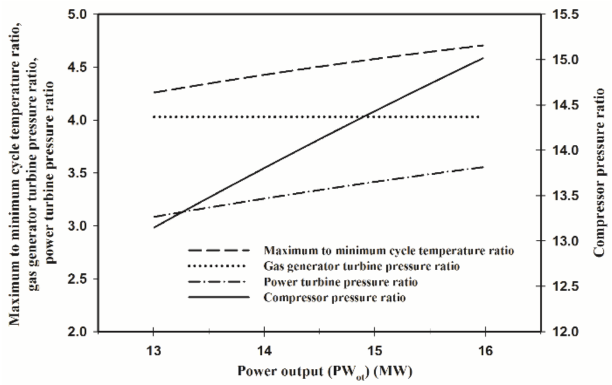

Fig. 14. Variation of pressure ratios under power load change.

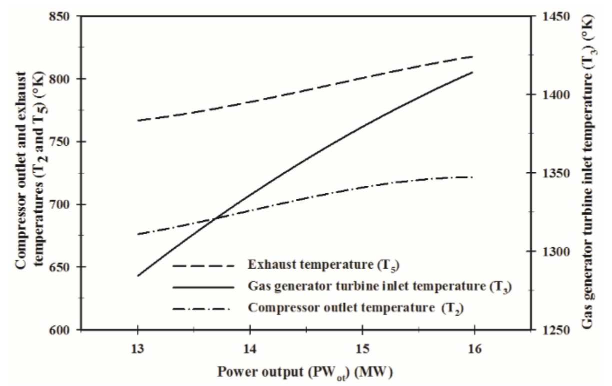

Fig. 15. Effect of power demands on various gas path temperatures.

be suggested to use more than one separate smaller engines, as each of them operates close to its design point.

Fig. 14 shows the trend of gas generator turbine pressure ratio at the constant rotational speed of 3000 RPM. As can be seen, the pressure ratio of gas generator turbine is constant, although the power output increases. This is because of choking that occurs in the power turbine and subsequently prevents any variation in pressure ratio of gas generator turbine.

Fig. 14 also shows the increase in both compressor and power turbine pressure ratios as power increase. In addition, it can be observed that the ratio of the combustion chamber outlet temperature to the compressor inlet temperature increases as the power output increases. This is mainly due to the increase in compressor pressure ratio. Note that since the power turbine pressure ratio is determined by the compression ratio of the gas generator and the efficiency of power turbine, it does not have any effect on the power developed by the gas turbine engine.

Fig. 15 also demonstrates the effect of power demand increase on various gas path temperatures. As it is observed, all temperatures increase proportionally with the load increase. However, the rate of compressor discharge temperature increment is slowing down by approaching to the design point. The probable reason for this issue is the fact that at this region the effect of pressure ratio increase on temperature is diminished by the effect of efficiency increase.

5. Conclusion

In order to quantifying the effect of mechanical load on the gas turbine performance, a direct comparison between the engine useful power output, its thermal efficiency, and the mechanical speed has been established with data obtained from a developed gas turbine part-load simulation model. Toward this goal, a complete set of engine design point key performance data was obtained using the information provided by the engine manufacturer and using the thermodynamic energy-based analysis. The scaling method was adopted to update the characteristic maps of a gas turbine component including compressor and turbines. Then, a matching process was employed to develop an off-design simulation model. The ambient condition and operation load are the input requirements of this model, whereas the pressure and temperature values through the gas path, air and fuel mass flow rates, gas generator speed, the isentropic efficiency of various components, and overall thermal efficiency of the engine are the output parameters. The graphical representation of data obtained using developed model demonstrates that in mechanical drive applications the gas turbine useful power output and its thermal efficiency changes with the mechanical speed. At higher mechanical speeds, the useful power output and thermal efficiency tend to be higher. The compressor rotational speed is a limiting factor as dictated to mitigate the risk of being overstressed as well as prevents stalling and surging. Hence, it is observed at higher mechanical speeds, the maximum achievable turbine useful power output is lower. As another consequence of this study, the thermal efficiency of gas turbine improves as the mechanical speed increases. However, the rate of this change decreases as the mechanical speed approaches the design point. At speeds far from design speed, the efficiency has a significant drop and, therefore, is a matter of concern. In addition, at any specific mechanical speed, the thermal efficiency decreases with the power that proves the gas turbines are most efficient under high load conditions. The proposed model and result provided can be integrated with the performance-based health assessment tool for advanced condition monitoring, prognostics, and diagnostics in mechanical drive applications.

Acknowledgement

The authors are grateful for the funding and facilities supported by Universiti Teknologi PETRONAS.

Nomenclature

Notations

P	: Pressure (bar(a))
T	: Temperature (K)
η	: Efficiency (-)
h	: Enthalpy (kJ/kg)
s	: Entropy (kJ/kg.K)

n : Molar flow rate (kmol/s)
PW : Power output (kW)
N : Rotational speed (RPM)
$\Delta\alpha$: Guide vane angle (degree)
M : Molecular weight (kg/kmol)
W : Work rate (kJ)
w : Mass flow rate (kg/hr)
γ : Isentropic index
Cp : Specific heat (kJ/kg.K)
R : Gas constant (kJ/kg.K)
LHV : Lower heating value (kJ/kg)
Q : Heat rate (J)
λ : Fuel-air mass ratio
PR : Pressure ratio
ΔP : Pressure loss (bar(a))
ΔQ : Heat loss (kJ)
Δw : Air bleed (kg/hr)

Abbreviations

C : Compressor
CC : Combustion chamber
GG : Gas generator
I : Intake
GGT : Gas generator turbine
PT : Power turbine
ED : Exhaust duct
CV : Control volume
VGV : Variable guide vanes

Subscripts

a : Air
f : Fuel
d : Design point
s : Isentropic
r : Reference engine
t : Target engine
pm : Performance map
ot : Output
oth : Overall thermal
$corc$: Corrected using curve
cor : Corrected
bl : Blow off
1 : Compressor inlet
2 : Compressor outlet
3 : Combustion chamber outlet
4 : Gas generator outlet
5 : Power turbine outlet

References

[1] P. Spina, Gas turbine performance prediction by using generalized performance curves of compressor and turbine stages, *Proc. of ASME Turbo Expo 2002: Power for Land, Sea, and Air*, Amsterdam, Netherlands (2002) 1073-1082.

[2] Y. Li, M. A. Ghafir, L. Wang, R. Singh, K. Huang and X. Feng, Nonlinear multiple points gas turbine off-design performance adaptation using a genetic algorithm, *Journal of Engineering for Gas Turbines and Power*, 133 (7) (2011) 07170.

[3] E. Tsoutsanis, N. Meskin, M. Benammar and K. Khorasani, Transient gas turbine performance diagnostics through nonlinear adaptation of compressor and turbine maps, *Journal of Engineering for Gas Turbines and Power*, 137 (9) (2015) 091201.

[4] D. E. Muir, H. I. Saravanamuttoo and D. Marshall, Health monitoring of variable geometry gas turbines for the Canadian Navy, *Journal of Engineering for Gas Turbines and Power*, 111 (2) (1989) 244-250.

[5] J. Kim, T. Song, T. Kim and S. Ro, Model development and simulation of transient behavior of heavy duty gas turbines, *Journal of Engineering for Gas Turbines and Power*, 123 (3) (2001) 589-594.

[6] F. Haglind, Variable geometry gas turbines for improving the part-load performance of marine combined cycles–Gas turbine performance, *Energy*, 35 (2) (2010) 562-570.

[7] J. Kurzke, *GasTurb 11: Design and Off-Design Performance of Gas Turbines*, Gas Turb11 (2007).

[8] H. Saravanamuttoo and B. MacIsaac, Thermodynamic models for pipeline gas turbine diagnostics, *Journal of Engineering for Gas Turbines and Power*, 105 (4) (1983) 875-884.

[9] A. M. Y. Razak, *Industrial gas turbines: performance and operability*, Elsevier (2007).

[10] M. Gobran, Off-design performance of solar Centaur-40 gas turbine engine using Simulink, *Ain Shams Engineering Journal*, 4 (2) (285-298) 2013.

[11] W. P. Visser and M. J. Broomhead, GSP, a generic object-oriented gas turbine simulation environment, *Proc. of ASME Turbo Expo 2000: Power for Land, Sea, and Air*, Munich, Germany (2000) V001T01A002-V001T01A002.

[12] H. Rashidzadeh, S. M. Hosseinalipour and A. Mohammadzadeh, The SGT-600 industrial twin-shaft gas turbine modeling for mechanical drive applications at the steady state conditions, *Journal of Mechanical Science and Technology*, 29 (10) (2015) 4473-4481.

[13] S. Bahrami, A. Ghaffari, S. H. Sadati and M. Thern, Identifying a simplified model for heavy duty gas turbine, *Journal of Mechanical Science and Technology*, 28 (6) (2014) 2399-2408.

[14] A. Lazzaretto and A. Toffolo, Analytical and neural network models for gas turbine design and off-design simulation, *International Journal of Thermodynamics*, 4 (4) (2001) 173-182.

[15] J. F. Sellers and C. J. Daniele, DYNGEN: A program for calculating steady-state and transient performance of turbojet and turbofan engines, *National Aeronautics and Space Administration* (1975) 7901.

[16] C. Kong, J. Ki and M. Kang, A new scaling method for component maps of gas turbine using system identification, *Journal of Engineering for Gas turbines and Power*, 125 (4) (2003) 979-985.

Appendix

A.1 The theory of auxiliary coordinates

Due two main reasons, a compressor map cannot be used directly in a performance calculation program. Firstly, in a part of the map, the speed lines may be vertical and it is not always possible to read efficiency from such a map at a given corrected speed and corrected flow rate. In addition, it is also not possible to read the map with given speed and pressure ratio because there might be two values for corrected flow at a given pressure ratio. This problem is addressed by using auxiliary coordinates, called β lines, intersecting the speed lines. The β lines are auxiliary coordinates and helps to read the map independent from the shape of the lines with given β and speed. In this way, for a given value of β and speed, the values of mass flow and pressure ratio, can be determined. This auxiliary coordinates, which have values between 0 and 1, can be represented by parabolic lines in the map, Fig. A.1.

In order to use the compressor maps using β lines, three tables need to be generated. The first table represents the compressor's corrected mass flow rate as a function of β and corrected speed. The next one represents pressure ratio as a function of β and corrected speed. And the last one represents isentropic efficiency as a function of β and corrected speed. In the turbine part, auxiliary β lines are not required. Thus, the corresponding maps can be transformed into two non-dimensional tables. These tables provide the non-dimensional mass flow rate and isentropic efficiency of the turbines as a function of pressure ratio and non-dimensional speed.

In all cases, a linear interpolation technique is adopted to determine the values at the intermediate points.

A.2 Design point model

In order to calculate the required design point performance data, following governing equations need to be solved. Toward this end, it is required to consider two individual control volumes, i.e. CV1 & CV2 presented in Fig. 5.

- Step A) To calculate T_{2d}.

1. Using P_{1d} and T_{1d}, calculate the value of h_{1d} and s_{1d}.

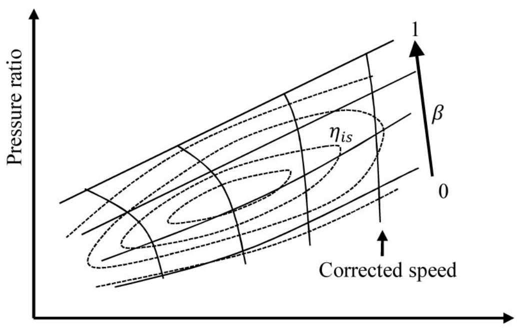

Fig. A.1. Utilization of β lines to read compressor map.

2. Set the value of s_{2sd} equal to s_{1d}.
3. Using s_{2sd} and P_{2d}, determine the value of h_{2sd} and T_{2sd}.
4. T_{2d} can be obtained using h_{2d} calculated Eq. (A.1).

$$h_{2d} = h_{1d} - \left[\frac{h_{2sd} - h_{1d}}{\eta_{scd}} \right]. \tag{A.1}$$

- Step B) To calculate m_{fd}.

By considering control volume enclosing compressor, combustion chamber and turbine, i.e. CV1, λ_d and subsequently m_{fd} can be achieved.

1. Use T_{fd} and T_{4d} to calculate h_{fd} and h_{4d}.
2. Calculate the heat wasted from control volume using Eq. (A.2):

$$\dot{Q}_{cv} = \Delta Q_{CC} \times LHV \times 0.94\ n_{1d}\lambda_d . \tag{A.2}$$

3. For CV1 heat balance is as following:

$$\dot{Q}_{cv} - \dot{W}_{cv} = n_{4d}h_{4d} - n_{fd}h_{fd} - n_{1d}h_{1d} . \tag{A.3}$$

Which leads to:

$$-\Delta Q_{CC} \times \lambda_d \times LHV + h_{1d} + \lambda_d \times h_{fd} - (\lambda_d + 1) h_{4d} = 0 . \tag{A.4}$$

4. Solve Eq. (A.4) to obtain λ_d.
5. Calculate the molar and mass flow rate using Eqs. (A.4) and (A.5) :

$$n_{fd} = \lambda_d n_{1d} \tag{A.5}$$

$$m_{fd} = \lambda_d m_{1d} M_a / M_f . \tag{A.6}$$

- Step C) To calculate T_{3d}.

Consider a control volume enclosing combustion chamber, i.e. CV2.

1. Determine P_3 using the assumed pressure drop across the combustion chamber.

$$P_{3d} = (1 - \Delta P_{CC}) \times P_{2d} . \tag{A.7}$$

2. Solve Eq. (A.8) to calculate h_{3d}.

$$-0.02 \times \lambda_d \times LHV + h_{2d} + \lambda_d \times h_{fd} - (\lambda_d +) h_{3d} = 0 . \tag{A.8}$$

3. By having h_{3d}, determine T_{3d} using thermodynamic charts.

- Step D) To calculate P_{4d} and P_{5d}.

4. Determine s_{3d} available values of P_{3d} and T_{3d}.
5. Set s_{4sd} equals to s_{3d}.
6. Assume a value for P_4 and by using s_{4sd}, calculate T_{4sd} and subsequently h_{4sd}.
7. Calculated h_{4d} using:

$$h_{4d} = h_{3d} - \left[\frac{h_{4sd} - h_{3d}}{\eta_{std}} \right]. \quad (A.9)$$

8. By having h_{4d}, determine T_4 using thermodynamic charts.
9. Compare T_4 calculated in steps 5 with available T_4 form manufacturer documents. If they do not agree, estimate a different T_4 and return to step 3.
10. Determine P_{5d} using Eq. (A.10).

$$P_{5d} = \left(1 + \Delta P_{ED}\right) \times P_{amb} . \quad (A.10)$$

A.3 Off-design model

Here, a demonstration of a basic matching procedure for a two-shaft gas turbine operating with a free power turbine is described. The required power output, mechanical speed, compressor inlet temperature and compressor inlet pressure are the model inputs.

1) T_{amb}, P_{amb}, PW_{ot}, and N_2 are considered as inputs.
2) $T_{1=}T_{amb}$ and $P_{1=}P_{amb}\left(1-\Delta P_I\right)$.
3) Estimate w_1, N_1, T_3, P_3 / P_4.
4) Calculate w_{1cor} and N_{1cor} using w_1, R_1 T_1 P_1 and N_1.
5) Use w_{1cor} and N_{1cor} and compressor curves, determine P_2 / P_1 and η_{12}.
6) Calculate P_2 using Eq. (A.11).

$$P_2 = P_1 \times P_2 / P_1 . \quad (A.11)$$

7) Considering Δw_{bl} and calculate the w_2.
8) Obtain T_2 using Eq. (A.12).

$$T_2 = T_1 - T_1 \times \eta_{12}\left[1-\left(P_1 / P_2\right)^{(\gamma-1/\gamma)}\right] \quad (A.12)$$

where γ is calculated using mean of T_1andT_2.
9) Calculate PW_C using Eq. (A.13).

$$PW_C = w_1 \times cp\left(T_2 - T_1\right) \quad (A.13)$$

where cp corresponding to the mean of $T_1$and T_2.
10) Use T_2, T_3, $T_3 - T_2$ and combustion charts to calculate the fuel flow, m_f.
11) Use ΔP_{CC} and P_2 to calculate the P_3.
12) Calculate w_3 using Eq. (A.14).

$$w_3 = w_2 + \Delta w_{bl-GGT} + m_f . \quad (A.14)$$

13) Determine w_{3cor} and N_{3cor} using w_3, R_3 T_3 P_3 and N_1.
14) Use estimated P_3 / P_4 and N_{3cor}, to determine w_{3corc} and η_{34} using the gas generator turbine curve.
15) Calculate T_4 using Eq. (A.15)

$$T_4 = T_3 - T_3 \times \eta_{34}\left[1-\left(P_4 / P_3\right)^{(\gamma-1/\gamma)}\right] \quad (A.15)$$

where γ is calculated using mean of T_3andT_4.
16) Obtain PW_{GGT} using Eq. (A.16).

$$PW_{GGT} = w_3 \times cp\left(T_3 - T_4\right) \quad (A.16)$$

where cp corresponding to the mean of T_3andT_4.
17) Calculate P_4 using Eq. (A.17).

$$P_4 = P_3 \times P_4 / P_3 . \quad (A.17)$$

18) Calculate w_4 using Eq. (A.18).

$$w_4 = w_3 + \Delta w_{bl-PT} . \quad (A.18)$$

19) Calculate w_{4cor} and N_{4cor} using w_4, R_4 T_4 P_4 and N_2.
20) Determine P_5 using Eq. (A.19).

$$P_1 = P_{amb}\left(1 + \Delta P_{ED}\right). \quad (A.19)$$

21) Using P_5 / P_4 and N_{4cor}, determine w_{4corc} and η_{45} using the power turbine curve.
22) Calculate T_5 using Eq. (A.20)

$$T_5 = T_4 - T_4 \times \eta_{45}\left[1-\left(P_5 / P_4\right)^{(\gamma-1/\gamma)}\right] \quad (A.20)$$

where γ is calculated using mean of T_4andT_5.
23) Calculate PW_{PT} using Eq. (A.21).

$$PW_{PT} = w_4 \times cpa\left(T_4 - T_5\right) \quad (A.21)$$

where cp is calculated using mean of T_4 and T_5.
24) If error between w_{3cor} and w_{3corc} is higher than threshold, estimate a different T_3 and return to step 10.
25) If error between PW_C and PW_{GGT} is higher than threshold, estimate a different P_3 / P_4 and return to step 14.
26) If error between w_{4cor} and w_{4corc} is higher than threshold, estimate a different T_3 and return to step 3.
27) If error between PW_{PT} and PW_{ot} is higher than threshold, estimate a different w_1 and return to step 3.

The acceptable error threshold for steps 21 to 24 should be determined during modeling. It is generally accepted that considering the high threshold reduces the accuracy of the model while the excessive reduction in this parameter will significantly increase the computational burdensome.

Mohammadreza Tahan received his B.Sc. and M.Sc. degrees in Mechanical Engineering from Engineering Faculty of Ferdowsi University, Mashhad, Iran, in 2005 and 2008, respectively. He has been a Senior Machinery Engineer in Nargan Engineers and Constructors for over 5 years before he joined Universiti Teknologi PETRONAS, Malaysia, in 2013 as a Research Assistant and Ph.D. student. His current research interests include design, implementation, and testing of real-time models for condition monitoring, health assessment, prognostics and diagnostics of rotating equipment.

Masdi bin Muhammad, C.Eng. (UK), CMRP, ASQ-Certified Reliability Engineer, is a Senior Lecturer in Mechanical Engineering Department and research cluster leader for Facility and Plant Engineering, Universiti Teknologi PETRONAS. He obtained his first and Master degrees, B.Sc. in Mechanical Engineering and M.Sc. in Manufacturing System Engineering, from Lehigh University, USA. His Ph.D. in Mechanical Engineering was obtained from UTP with research on Reliability Model for Repairable Systems with Multi-State Degradation. He is actively involved in consultation work and training on asset reliability and integrity for oil and gas companies.

Zainal Ambri Bin Abdul Karim currently serves as an Associate Professor at the Mechanical Engineering Department of Universiti Teknologi PETRONAS and has been with the department for almost 17 years. He obtained his B.Sc. in Marine Engineering (USA) and later read Automotive Engineering to Ph.D. level (UK). He had conducted several short courses for the Accelerated Capability Development for PETRONAS Engineers Skill Group 12 which include Design, Operation, Maintenance and Inspection of Steam Boilers, Internal Combustion Engines, and Automotive Engineering. In addition, he also contributed to other short-courses such as Centralized Distributed Cooling System and Thermal Power Plant Efficiency & Heat Rate Improvement. He is an active reviewer for several international journals while having published more than 30 journal articles. His research interests include combustion analysis, energy optimization, marine engineering, power plant engineering and internal combustion engines.